

Thin betatron radiators for more efficient x-ray generation

V. V. Kaplin^{a)} and S. R. Uglov

Nuclear Physics Institute, Tomsk Polytechnic University, P.O. Box 25, Tomsk 634050, Russia

O. F. Bulaev, V. J. Goncharov, and A. A. Voronin

Institute of Introscopy, Savinikh st. 3, Tomsk 634034, Russia

M. A. Piestrup^{b)} and C. K. Gary

Adelphi Technology, Incorporated, 2181 Park Boulevard, Palo Alto, California 94306

(Received 4 October 2000; accepted for publication 22 October 2001)

We present experimental evidence that electrons of modest energy are making multiple passes through thin targets placed inside a betatron toroid, thus increasing their bremsstrahlung emission efficiency. Thin Cu, Be, W, and Mylar targets of thicknesses between 10^{-5} to 3.5×10^{-3} radiation lengths were used. The number of passes through the thin radiators were obtained using either the bremsstrahlung photon densities or angular distributions. The number of passes of 33-MeV electrons through the thin radiators was estimated to be 590 for a 1- μm -thick Cu foil, 171 for 5- μm Cu, 30 for 15- μm Cu, 200 for 20- μm Be, 51 for 60- μm Be, 20 for 200- μm Be, 460 for 3- μm -thick Mylar, and 123 for 2- μm W foils. The multiple-pass effect can be useful for increasing the efficiency of novel x-ray sources such as transition and parametric radiators. © 2002 American Institute of Physics. [DOI: 10.1063/1.1427302]

I. INTRODUCTION

Recycling electrons through thin targets may enable the production of intense, quasimonochromatic x-rays from low-current cyclical accelerators. Previous experiments at the Tomsk synchrotron used 900-MeV electrons to demonstrate that an electron beam can be recycled through both transition and parametric x-ray radiators.¹ Recycling was also demonstrated in the electron storage ring at the Saskatchewan Accelerator Laboratory using 118–252-MeV electrons and transition radiators.² Both of these experiments showed that multiple passes of the electron beam through thin targets can remarkably increase the efficiency of x-ray production without significantly changing its spectral and angular distributions.

The possibility of a similar effect using a betatron at more modest energies was shown by means of computer simulation.³ This simulation was based on the magnetic-field parameters and toroid sizes of 6- and 35-MeV betatrons available at the Tomsk Research Institute of Introscopy (RII). The mean number of electron passes through the target was calculated as a function of the target thickness and position within the betatron chamber. The mean number of passes can be very large in the case of thin bremsstrahlung targets⁴ indicating that novel sources, such as crystalline^{5,6} or multilayered⁷ radiators, can be used as internal targets for intense,⁶ tunable, collimated, and monochromatic⁵ x-rays.

In general, x-ray production in novel sources is proportional to both radiator thickness and the electron current passing through it. However, since the length of a radiator is limited by self-absorption of the x-rays, increasing the aver-

age current via recycling may be the best way to increase the overall production efficiency. Modern, modest-energy betatrons, such as manufactured by RII and Adelphi Technology, Inc., are small and inexpensive. The researchers envision a “table-top synchrotron,” a compact quasimonochromatic x-ray source, capable of replacing large expensive synchrotrons for some applications such as mammography⁸ and lithography.⁹ The aim of the present work is to demonstrate feasibility by observing multiple passes of electrons incident on thin target foils in a betatron. Some early results of this work have been published.⁴

II. EXPERIMENTAL APPROACHES AND APPARATUS

By measuring either the γ -ray angular distributions or relative photon densities, we estimated the number of passes of the electrons through thin targets. The electron spatial distribution at the target also gave an indirect indication of multipasses.⁴ These methods were used since more direct means, such as a measurement of the pulse structure of the electron beam as it passes through the radiator, would be difficult, if not impossible. The cyclical path of the electron beam is continuous around the betatron toroid during the acceleration pulse of the betatron, and, thus, there is no micropulse structure to measure as electrons pass through the radiator.

Our simulations of the dynamics of electrons in a betatron showed that the main effects of recirculation consist in the increase of the total yield of radiation, broadening of the angular distribution of the electron beam, and a spread of the spatial distribution of the electrons on the target surface.³ For a thin target, the increase in radiation production over that of a single pass is proportional to the mean number of passes, N ; and the broadening of the angular distribution is propor-

^{a)}Electronic mail: kaplin@npi.tpu.ru

^{b)}Electronic mail: melpie@adelphitech.com

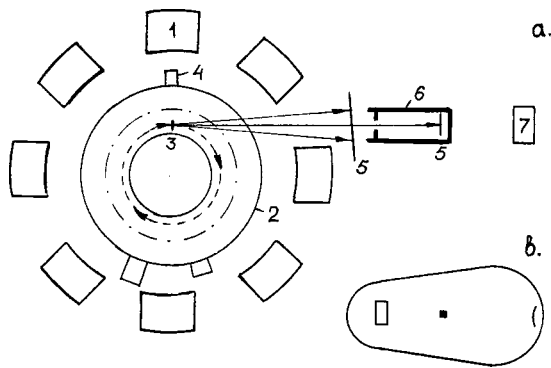


FIG. 1. (a) Experimental arrangement: 1—betatron magnet, 2—betatron chamber (toroid), 3—internal target, 4—system for mechanical translation of the target in radial direction, 5—x-ray film, 6—camera-obscura, 7— γ -ray detector. (b) Cross section of the ceramic toroid of the 35-MeV betatron. The dark square shows a possible position of the target inside the equilibrium orbit ($R_0=245$ mm) of the accelerated electron beam; the arc shows the injector position.

tional to the square root of N . Thus, by measuring both the γ -ray spatial distribution and intensity, we were able to obtain estimates of N .

The experimental arrangement is shown in Fig. 1(a). We used the 35-MeV Tomsk betatron model number B-35, (1), whose characteristics were used in the simulations.³ After the injection of 60-keV electrons in a ceramic toroid (2) and after accelerating the electrons to the required energy by means of the rising magnetic field, the electrons were dumped on an internal target (3) by the influence of an additional magnetic field of 30- μ s duration. The additional magnetic field changed the betatron condition, moving the equilibrium orbit inward so that the electrons struck the edge of the internal target. The thin target was supported by a holder at radial position R_t inside the initial electron-beam orbit. The target could be mechanically translated (4) perpendicular to the electron-beam orbit. The repetition rate of the accelerator was 50 Hz, and the single pass current of electrons dumped on the target was about 20 nA. The divergence of the electron beam was less than 0.3 mrad, and the electron energy spread was 0.5%. The electron energy could be varied within a range of 15–33 MeV by changing the maximum value of the guiding magnetic field.

The cross section of the 35-MeV betatron chamber (toroid) is shown in Fig. 1(b). In our previous work, we simulated the recycling effect for internal targets positioned inside and outside the equilibrium orbit ($R_0=245$ mm) of the accelerated electrons.³ We found the inside position to be the most promising for giving the largest number of passes; hence, we placed targets at various inside positions.

The bremsstrahlung generated from the various targets was transmitted through the 5-mm ceramic wall of the betatron toroid to expose x-ray film D-4 (5), which was placed 560 mm from the target. The film was used to measure the angular distribution of bremsstrahlung γ -rays.

The distribution of the electrons hitting the target surface was imaged using a camera obscura (pin-hole camera) (6) placed at a distance of 600 mm from the target. The diameter of the pin hole was 50 μ m, the lead iris thickness was 4 mm and the camera length was 400 mm. X-ray film with an area

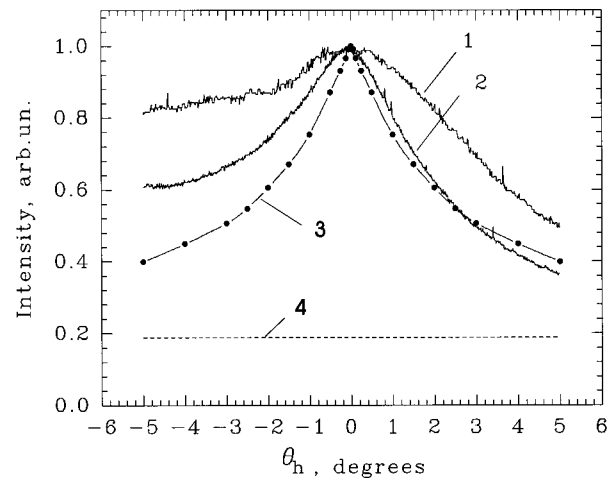


FIG. 2. Horizontal angular distributions of γ -rays generated by 15- and 33-MeV electron beams in a 1.3-mm-thick W target placed at position $R_t=205$ mm inside the betatron toroid (curves 1 and 2, respectively). Curve 3 shows the calculated distribution of bremsstrahlung and the dashed line 4 shows the expected background level for a 33-MeV beam.

of 30×30 mm² was placed at a distance of 350 mm from the iris to obtain images of the electron beam spot on the target.

We used an ionization chamber (7) with a diameter of 50 mm and a volume of 20 cm³ placed at a distance of 1500 mm from the target to control the exposure time of the film and, later, to obtain the relative intensities of the bremsstrahlung. The grayscale information from the photographic images was digitized using a scanner. For more about this technique, see Ref. 4.

III. EXPERIMENTAL RESULTS

A. Thick W target

We measured the relative photon density and the angular distribution of γ -rays generated from a single pass through a thick target in order to compare with the case of multiple passes through thin targets. The target was a 1.3-mm-thick W plate with a surface area of 5×25 mm².

We first measured the relative photon density for three target positions to determine the influence of the position on electron capture during acceleration and to estimate the optimum toroid position of the radiator. Any target placed inside the betatron chamber should decrease the effective cross section of the chamber for capturing the injected low-energy electrons. The measurements carried out for 33-MeV electrons using the ionization detector [(7) in Fig. 1] showed that the γ -ray yields for the target positions $R_t=205$, 210, and 215 mm correspond to the ratio of 1: 0.8 : 0.47 [normalized to position $R_t=205$ cm]. Thus, moving the target towards the equilibrium electron orbit reduces the percentage of 60-keV electrons captured for acceleration because the effective cross section of the toroid is decreased. The majority of the injected electrons hit the target and were not accelerated when the target was placed close to the initial electron orbit, resulting in the betatron beam current decreasing sharply.

Using the film image technique described, we then obtained the angular distribution of the γ -rays from the thick target.⁴ Figure 2 shows the horizontal profiles of the angular

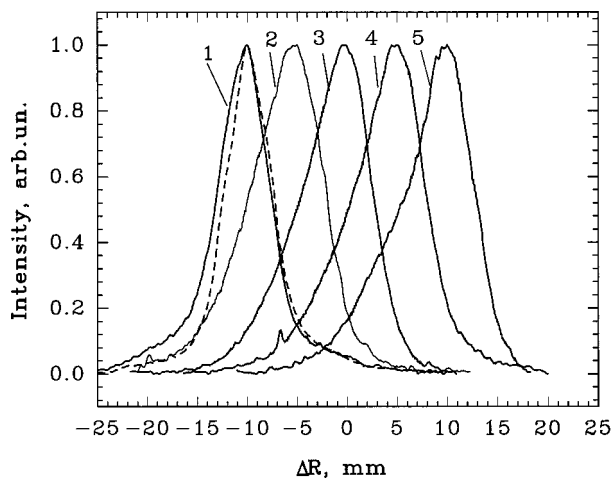


FIG. 3. Horizontal profiles of the beam spot of 33-MeV electrons on a 15- μm Cu target surface for target positions $R_t=195, 200, 205, 210,$ and 215 mm (curves 1–5, respectively) compared with a 1.3-mm-W target (dashed curve).

distributions of γ -rays generated by 15- and 33-MeV electrons in the 1.3-mm-thick W target placed at the position $R_t=205$ mm. The width of the profiles decreases with increasing electron-beam energy. The calculated curve shows the bremsstrahlung angular distribution, which was obtained using the Electron PHoton CAscade (EPHCA) computer code.¹⁰ The calculation was carried out for 33-MeV electrons, taking into account the transmitting of the γ -rays through the 5-mm ceramic wall of the toroid. The experimental and calculated data are in general agreement if the level of bremsstrahlung background is taken as shown by the horizontal dashed line. Asymmetries of the distributions reflect the fact that individual electrons incident on the thick target edge produce bremsstrahlung with asymmetric spatial distribution.⁴

B. Thin Cu targets

In the first experiments with thin targets, we used 15- and 5- μm -thick Cu foils with the horizontal and vertical dimensions of 10 and 38 mm, respectively. Figure 3 shows the horizontal beam-spot profiles of 33-MeV electrons on a 15- μm Cu target at positions $R_t=195, 200, 205, 210,$ and 215 mm (curves 1–5) along with the profile obtained using the thick 1.3-mm W target (dashed curve). It is seen that even for the target position farthest from the equilibrium electron orbit (curve 1), the beam spot is larger than that of the thick W target. This is due to the repeated passes of the electrons through the thin Cu target.

As the thin Cu target was moved toward the equilibrium orbit, the spatial distribution of electrons widened further. Electrons initially strike the target near the edge closest to the beam, but when the target is close to the equilibrium orbit, recirculated electrons strike the target at significant distances from the edge due to multiple passes. This is most likely because the radii of electron orbits decreases from pass to pass due to energy losses. The curves show that multiple recirculation of electrons through the target is most effective for target positions closest to the equilibrium electron orbit.

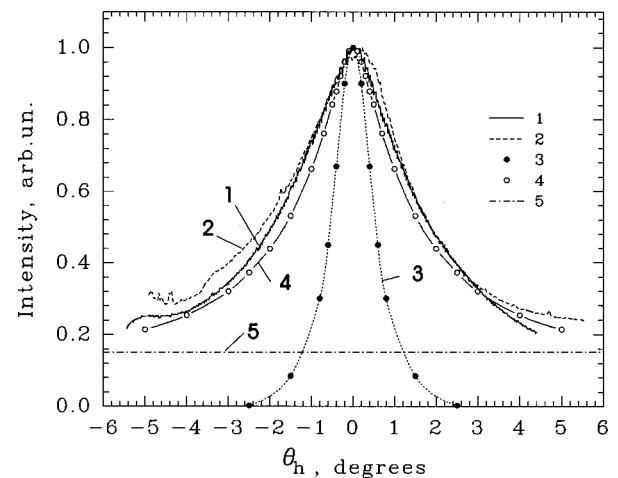


FIG. 4. Horizontal profiles of the angular distributions of γ -rays generated by 33-MeV electrons passing through 15- and 5- μm -thick Cu targets placed at $R_t=210$ mm (curves 1 and 2, respectively). Curve 3 shows the calculated distribution of γ -rays generated by 33-MeV electrons in a 15- μm -thick Cu foil for a single pass. Curve 4 is calculated with the EPHCA codes for a 450- μm Cu target, which equivalent to $N=30$ passes. Thus, this estimate (4) matches the experimental (2) well. The level of background is given by the horizontal dashed-point line (curve 5)

The horizontal profiles of the angular distributions of γ -rays generated by 33-MeV electrons in the 15- and 5- μm Cu targets at $R_t=210$ -mm are shown in Fig. 4 (curves 1 and 2, respectively). For comparison, the Fig. 4 shows the calculated angular distribution, curve 3, of γ -rays generated by a perfectly collimated 33-MeV electron beam on a single pass through a 15- μm Cu foil. We see that the experimental distribution of γ -rays (curve 2) is much broader than the calculated one (curve 3) for a single pass. This implies that the electrons passed many times through the target, and, indeed, we estimated N using the value of the full width half maximum (FWHM) of the experimental angular distribution. The angular spread of the electron beam caused by uncorrelated scattering from successive passes through the thin target adds in quadrature, giving a total spread which is proportional to the square root of the product of number of passes, N , and target thickness, t .

For approximating the number of passes N , we compared our experimental bremsstrahlung angular distributions with the calculated distributions obtained for a thick target using the EPHCA code. We assumed that the distribution is the same from a single pass of a thick target of thickness T and many passes through a thin target of thickness t , if $T=Nt$. Thus, in Fig. 4, we present the distribution of bremsstrahlung (curve 4) calculated with the EPHCA code for a 450- μm Cu target equivalent to $N=30$. There is good agreement between theory (curve 4) and experiment (curve 2) for the 15- μm target if we take the level of background radiation as given by the horizontal dashed-point line (curve 5). Therefore, one can conclude that the mean number of passes is about 30. The distribution measured for the 5- μm Cu foil is even broader; and using the simulation we estimate the mean number of passes to be greater than 90.

Such a determination of the numbers of passes N of the recirculated beam does not take into account the focusing properties of the magnetic field of the betatron. But these

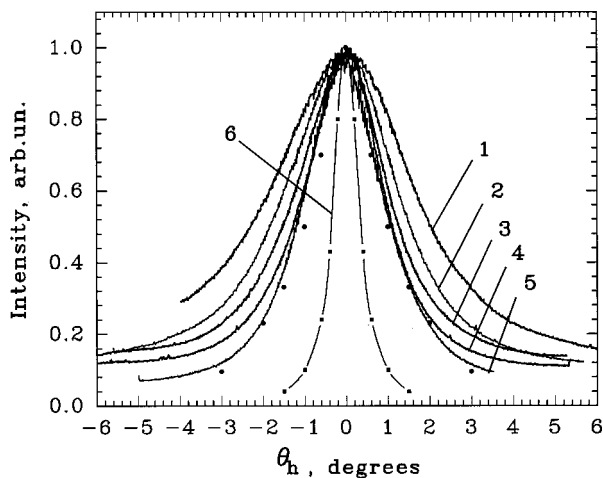


FIG. 5. Horizontal profiles of the angular distributions of γ -rays generated by 15-, 20-, 25-, 28.5-, and 33-MeV electron beams in a 20- μm -thick Be target placed at position $R_t=210$ mm inside the betatron toroid (curves 1–5, respectively). Curve 6 and the points just under curve 5 show the calculated distributions of γ -rays generated by 33-MeV electrons in the 20- μm and 4-mm-thick Be targets for a single pass, respectively.

results confirm that recycling occurs and that the mean number of passes can be very large for sufficiently thin targets.

C. Thin Be foils

We continued the measurements of multipass characteristics using 20-, 60-, and 200- μm -thick Be targets with horizontal and vertical dimensions of 10 and 20 mm, respectively. We measured the energy dependence of the angular distribution of γ -rays generated in these Be foils and dependence on target position, but our main aim was to measure the relation between the number of passes and the target thickness.⁴ Be has a lower density and much greater radiation length than Cu, which leads to a different ratio of ionization to radiation energy losses; and, hence was expected to facilitate a large numbers of passes.

Figure 5 shows the horizontal profile of angular distributions of γ -rays generated by 15-, 20-, 25-, 28.5-, and 33-MeV (curves 1–5, respectively) electrons in a 20- μm Be target placed at $R_t=210$ mm in the betatron toroid. It can be seen that the spot size decreases when the electron energy increases. Curve 6 shows the theoretical distribution of γ -rays from 33-MeV electrons on a single pass, which was calculated using the EPHCA code for a 20- μm target. The points under curve 5 show the calculated distribution from a single pass through a 4-mm Be target without taking into account the dimensions of the beam spot on the target. Better agreement between the experimental distribution from multiple passes through a 20- μm target and a theoretical curve obtained for a 4-mm Be target (points under curve 5) can be achieved if one takes the beam-spot size and beam divergence into account. In this case, the value of the FWHM of the theoretical distribution is about 2.24° , while the measured FWHM = 2.3° . Again, if we assume that the total target thickness traversed by the electrons, either on many passes through the thin target or on one pass through the thick target, is equal (i.e., $T=Nt$), then the mean number of passes is approximately 200 for the 20- μm target.

TABLE I. The number of passes for various foils.

Foil (mm ²)	t (μm)	Number of passes for 33-MeV electrons		
		Using the Bs angular distribution	Using the Bs photon densities	Using thermal damage
Be (10 \times 20)	20	200
	60	51
	200	18
Cu (6 \times 8)	1	...	590 (377 at 20 MeV)	...
Cu (8 \times 38)	5	>90	171	...
Mylar (10 \times 38)	15	30
Mylar (10 \times 38)	3	...	460	250–500
W (8 \times 20)	2	...	123	...

We also obtained the images of 15-, 20-, and 33-MeV electron-beam spots on the 20- μm Be target placed at $R_t=210$ mm. The beam spot became slightly larger for decreasing electron energies, but in all cases it was much broader than that obtained for the thicker and denser 1.3-mm W target placed at the same position. Again this implies multiple passes through the thinner Be target. The images of the beam spots on the surface of the 20- μm Be target placed at $R_t=205, 210, 215,$ and 220 mm showed that the recycled electron beam profile did not strongly depend on the target position in this range.⁴ The behavior of the electron-beam spot for the 60- and 200- μm targets with changing position and electron energy is similar to the behavior for the 20- μm target.⁴

The measured angular distributions of γ -rays generated by 33-MeV electrons in a 20- μm Be target placed at positions $R_t=210$ and 215 mm became broader as the target was moved towards the equilibrium orbit. The FWHMs of the distributions were about 2.3° and 2.5° , respectively, implying that the number of passes increased when the target was moved towards the equilibrium electron orbit.

The FWHMs of the measured angular distributions obtained for the 60- and 200- μm targets were slightly smaller than those obtained with the 20- μm target. From the FWHM values, we estimated the number of passes for the 200-, 60-, and 20- μm -thick targets to be 18, 51, and 200 (summarized in Table I). Using these values of N , the ratio of the products Nt is about 1.3:1:1.18, respectively. Thus, the product Nt does not vary significantly with target thickness over this range of target thicknesses.²

D. Thin Mylar target

We also investigated multiple passes through a 3- μm Mylar ($\text{C}_5\text{H}_4\text{O}_2$) target. The horizontal and vertical target dimensions were 10 and 38 mm, respectively. We found that the profile of 33-MeV electron-beam-spot images on the surface of the 3- μm Mylar target placed at position $R_t=210$ mm was broader than that for the Be targets. This implied that the number of passes for the Mylar target was larger than of the 20- μm Be foil. We also found that the angular distribution of γ -rays generated by 33-MeV elec-

trons in the 3- μm Mylar target placed at position $R_t = 210$ mm was a little broader than that for the 20- μm Be foil, which again implied more passes.

The increasing number of cycles through the Mylar target was sufficient to partially melt it when the target was placed at $R_t = 215$ mm. Upon inspection, the target edge was deformed and slightly thicker. The bremsstrahlung yield was observed to decrease by a factor of about 0.4 times. The calculated beam current necessary to melt a Mylar target is about 5–10 μA . Therefore, one can roughly estimate that the mean number of electron passes through the Mylar target is 250–500 because the current of the electron beam incident on the target is about 0.02 μA .

E. Photon density ratio

We obtained the ratio of photon densities generated by electrons for multiple and single passes by comparing the fluxes from thin Mylar, Cu, and W foils with either a 1.5-mm-thick Cu or a 1.3-mm-thick W target. This permitted us to obtain another estimate of the number of passes through the thin targets.

A target holder was constructed to allow the thin and thick targets to be interchanged without opening the betatron, thus permitting identical experimental conditions for the measurements. The detector (7) used for the flux measurements had an aperture of 1.65° allowing the measurement of the angular photon densities of the bremsstrahlung.

In the case of a 3- μm Mylar foil we used a 1.5-mm-thick Cu target to compare the bremsstrahlung flux ratio measured by 33-MeV electrons. The horizontal and vertical dimensions of the targets were 6 mm and 38 mm, respectively. We obtained a ratio between the photon densities of γ -rays from the thin and thick target of 0.33, while the ratio of their thicknesses (in units of radiation length) is about 10^{-4} . Assuming that the photon density of γ -rays is proportional to the function $\ln(968T)$ in the target thickness range of $T = 10^{-1}$ to 10^{-3} radiation lengths¹¹ and that $T = Nt$, we estimated N for the 3- μm Mylar foil to be about 460, comparing well with that from the thermal-damage estimate of 250 to 500 obtained above (summarized in Table I).

Using a 5- μm -Cu foil with the horizontal and vertical dimensions of $8 \times 38\text{-mm}^2$ and the aforementioned 1.5-mm Cu plate, we obtained a ratio of the angular densities of γ -rays from the thin and thick targets of 0.88, while the ratio of their thicknesses was about 3.33×10^{-3} . From this we estimated a mean number of electron passes through the 5- μm -Cu foil to be approximately 171, higher than the estimate of >90 obtained by the angular distribution (summarized in Table I).

Using a 1- μm -Cu foil with the horizontal and vertical dimensions of $7 \times 8\text{ mm}^2$, we obtained a ratio of the angular densities of γ -rays from this target and from 1.5-mm-Cu plate of 0.8 and 0.7 at the electron energies of 33 and 20 MeV, respectively. It gives the estimations of the number of passes through the foil of 590 and 377, respectively (Table I).

In the case of a 2- μm -W foil with the dimensions of $8 \times 20\text{ mm}^2$, we obtained the ratio of the fluxes of bremsstrahlung generated in this foil and in the thick W plate of 0.83 for

33-MeV electrons. The estimated mean number of passes is about 123.

IV. DISCUSSION

A summary of the estimates of the number of passes obtained by measuring bremsstrahlung photon density or angular distribution through different radiators are given in Table I. These estimates show that 15–33-MeV electrons can recirculate many times through internal targets with thicknesses of 10^{-5} to 3.5×10^{-3} radiation lengths, and that the fluxes of bremsstrahlung generated by electrons recycled through thin targets are almost the same as in the case of thick ones. As was found in Ref. 2 for higher electron energies in a synchrotron, the product, Nt does not strongly depend on the target thickness and, in the present research, is approximately a constant for $t < 10^{-3}$ radiation lengths. Thus, the number of target passes can be large for thin targets, such as those necessary for efficient production of low-energy x-rays. This is important since the effective current of electrons through the internal target, in comparison to a single-pass system, is proportional to the mean number of electron passes. Such targets might most appropriately be used for the production of low-energy radiation since absorption in the target material limits the target thickness. Indeed, recycling increases the portion of the beam energy that can be used for the production of x-rays, regardless of target thickness.

Finally, electron recycling causes a spread of the angular distribution of bremsstrahlung generated in a thin target and also a spread of the electron-beam spot on the target surface. The scattering of electrons and their energy losses in the target cause the beam emittance to increase during recirculation. The spread of the spot of the recirculated electron beam on the target depends on thickness, material, and electron energy. It also depends strongly on the target position which is close to the minimal radius $R = 180$ mm of the betatron toroid.

ACKNOWLEDGMENTS

This work was supported by the Russian Foundation of Basic Research and by the United States National Institutes for Health under the Small Business Innovation Research (SBIR) program (Grant Nos. 1-R43-RR11647-02 and 1-R43 CA86545-01).

¹M. Y. Andreyashkin, V. V. Kaplin, M. A. Piestrup, S. R. Uglov, and V. N. Zabaev, *Appl. Phys. Lett.* **72**, 1385 (1998).

²M. A. Piestrup, L. W. Lombardo, J. T. Cremer, G. A. Retzlaf, R. M. Silzer, D. M. Skopik, and V. V. Kaplin, *Rev. Sci. Instrum.* **69**, 2223 (1998).

³V. V. Kaplin, L. Lombardo, A. A. Mihal'chuk, M. A. Piestrup, and S. R. Uglov, *Nucl. Instrum. Methods Phys. Res. B* **145**, 244 (1998).

⁴V. V. Kaplin, S. R. Uglov, O. F. Bulaev, V. J. Goncharov, M. A. Piestrup, and C. K. Gary, *Nucl. Instrum. Methods Phys. Res. B* **173**, 3 (2001).

⁵K.-H. Brenzinger, B. Limburg, H. Backe, S. Dambach, H. Euteneuer, F. Hagenbuck, C. Herberg, K. H. Kaiser, O. Kettig, G. Kube, W. Lauth, H. Schope, and T. Walcher, *Phys. Rev. Lett.* **79**, 2462 (1997).

⁶S. Asano, I. Endo, M. Harada, S. Ishii, T. Kobayashi, T. Nagata, M. Muto, K. Yshida, and H. Nitta, *Phys. Rev. Lett.* **70**, 3247 (1993).

⁷V. V. Kaplin, S. R. Uglov, V. N. Zabaev, M. A. Piestrup, C. K. Gary, and M. J. Fuller, *Appl. Phys. Lett.* **76**, 3647 (2000).

⁸M. A. Piestrup, Xizeng Wu, V. V. Kaplin, S. R. Uglov, J. T. Cremer, D. W. Rule, and R. B. Frioito, *Rev. Sci. Instrum.* **72**, 2159 (2001).

⁹M. A. Piestrup, M. W. Powell, J. T. Cremer, L. W. Lombardo, V. V. Kaplin, A. A. Mihal'chuk, S. R. Uglov, V. N. Zabaev, D. M. Skopik, R. M. Silzer,

and G. A. Retzlaff, *Proc. SPIE* **3331**, 450 (1998).

¹⁰V. Bespalov, EPHCA (Electron PHoton CAscade) codes, Tomsk Polytechnic University, Tomsk 634050, Russia.

¹¹H. V. Koch and J. W. Motz, *Rev. Mod. Phys.* **31**, 920 (1959).